iScience

CellPress
OPEN ACCESS

Article

Thermal acclimation uncovers a simple genetic basis of adaptation to high temperature in a cosmopolitan pest

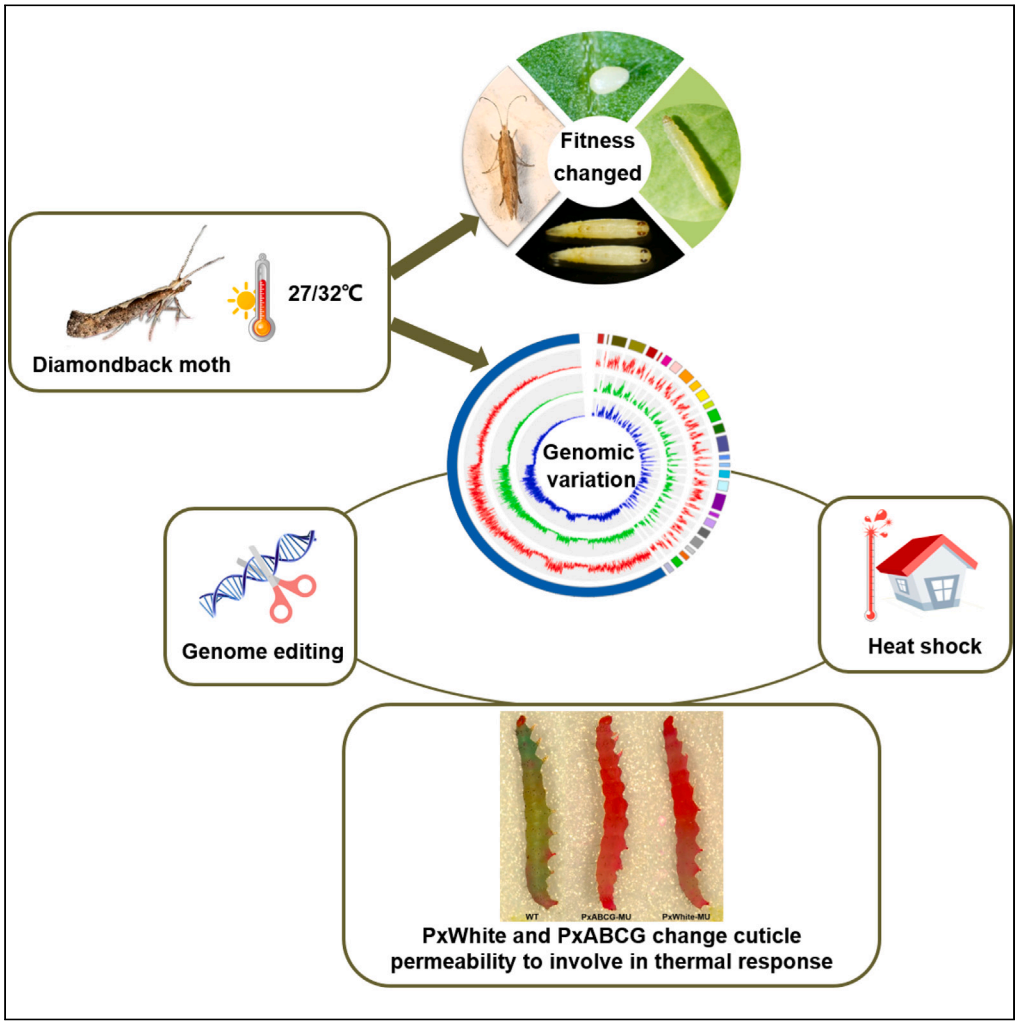

Shijun You, Gaoke Lei, Huiling Zhou, ..., Geoff M. Gurr, Minsheng You, Yanting Chen

fafucyt@126.com

Highlights

DBM can rapidly adapt to thermal environment

A series of genes potentially involved in thermal adaptation of DBM

ABCG transporter genes play an important role in thermal adaptation of DBM

PxWhite and *PxABCG* change cuticle permeability to involve in thermal response of DBM

You et al., iScience 27, 109242
March 15, 2024
https://doi.org/10.1016/j.isci.2024.109242

iScience

CellPress
OPEN ACCESS

Article

Thermal acclimation uncovers a simple genetic basis of adaptation to high temperature in a cosmopolitan pest

Shijun You,[1,2,3] Gaoke Lei,[1,2,3] Huiling Zhou,[1,2,3] Jianyu Li,[1,2,3] Shaoping Chen,[1,2,3] Jieling Huang,[1,2,3] Liette Vasseur,[1,2,4] Geoff M. Gurr,[1,2,5] Minsheng You,[1,2,3] and Yanting Chen[1,2,3,6,*]

SUMMARY

Understanding a population's fitness heterogeneity and genetic basis of thermal adaptation is essential for predicting the responses to global warming. We examined the thermotolerance and genetic adaptation of *Plutella xylostella* to exposure to hot temperatures. The population fitness parameters of the hot-acclimated DBM strains varied in the thermal environments. Using genome scanning and transcription profiling, we find a number of genes potentially involved in thermal adaptation of DBM. Editing two ABCG transporter genes, *PxWhite* and *PxABCG*, confirmed their role in altering cuticle permeability and influencing thermal responses. Our results demonstrate that SNP mutations in genes and changes in gene expression can allow DBM to rapidly adapt to thermal environment. ABCG transporter genes play an important role in thermal adaptation of DBM. This work improves our understanding of genetic adaptation mechanisms of insects to thermal stress and our capacity to predict the effects of rising global temperatures on ectotherms.

INTRODUCTION

As small ectotherms, insects are profoundly affected by variation in air temperatures, influencing their survival, distribution, and population dynamics.[1,2] Ongoing global warming is predicted to increase mean temperatures and the frequency of heat waves.[3] Climate change has already had significant biological impacts on insects, including affecting physiological, behavioral, and life history traits, shifting distribution and phenology and altering population dynamics and changing biotic interactions.[2,4,5] The susceptibility of insects to extreme temperature events is largely determined by degree of thermotolerance and temperature acclimation.[5–8] In response to increasing environmental temperature, species may adapt with greater basal thermal tolerance (genetic/evolutionary responses), greater induced thermal tolerance (plastic response), and more efficient thermoregulation behavior.[9]

In the face of global climate change, understanding the genetic adaptability of species is key to predicting their future distribution and impacts. By studying the genes involved in regulating the expression of thermotolerant phenotypes and the genes that harbor allelic variation that contributes to differences in thermal plasticity, researchers can identify the genetic basis of thermal adaptation that allows organisms to adapt to different temperatures.[10] For example, when *Drosophila simulans* is exposed to high temperatures for 60 generations, the metabolic systems are modified to adapt to the new thermal environment.[11]

Currently, transcriptomic approaches are used to study environmental effects on gene expression.[12,13] Although transcriptomics can provide valuable insights, differences in gene expression have not been able to provide direct evidence for adaptive evolution in organisms.[10] Changes in allele frequency within a population should provide the raw material for selection to drive adaptive evolution.[10,14] Several genes, particularly heat shock proteins, have been implicated in thermal tolerance mechanisms.[12,15,16] Notably, a more robust HSP response in *Drosophila melanogaster* compared to *Drosophila subobscura* contributes significantly to the enhanced heat tolerance of *D. melanogaster*.[16] Various strains of *D. melanogaster* have been the subject of genomic studies to investigate thermal adaptation, thermal plasticity, and thermal tolerance.[17] This previous work provides a platform for investigating similar phenomena in other insect species.

[1]State Key Laboratory of Ecological Pest Control for Fujian-Taiwan Crops, Institute of Applied Ecology, Fujian Agriculture and Forestry University, Institute of Plant Protection, Fujian Academy of Agricultural Sciences, Fuzhou 350002, China
[2]Joint International Research Laboratory of Ecological Pest Control, Ministry of Education, Fuzhou 350002, China
[3]Ministerial and Provincial Joint Innovation Centre for Safety Production of Cross-Strait Crops, Fujian Agriculture and Forestry University, Fuzhou 350002, China
[4]Department of Biological Sciences, UNESCO Chair on Community Sustainability, Brock University, St. Catharines, ON L2S 3A1, Canada
[5]Gulbali Institute, Charles Sturt University, Orange, NSW 2800, Australia
[6]Lead contact
*Correspondence: fafucyt@126.com
https://doi.org/10.1016/j.isci.2024.109242

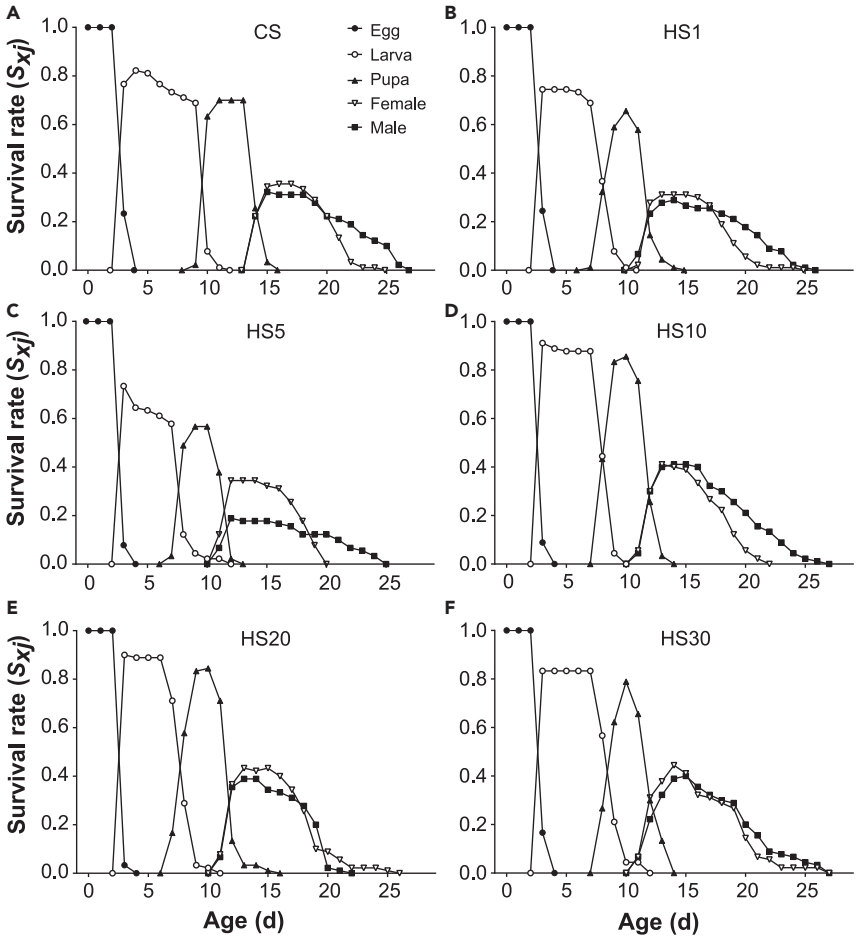

Figure 1. Age-stage specific survival rate (*Sxj*) of the control strain (CS) and hot-evolved strain (HS) of *P. xylostella*

CS (A) represents DBM kept under favorable temperature; and HS1(B), HS5 (C), HS10 (D), HS20 (E) and HS30 (F) represent the 1st, 5th,10th, 20th, 30th generations of DBM kept under high temperature.

The diamondback moth (DBM, *Plutella xylostella*) is a major pest of cruciferous vegetables and wild plants. Previous studies have shown that the diamondback moth exhibits significant genetic plasticity and high levels of genomic variation, allowing it to adapt rapidly to different environments.[18] In previous work, we have provided evidence for the genetic basis of climatic adaptation and predicted that most DBM populations have a high tolerance to future climates.[19] Previous analyses were based on genomic data from field DBM populations collected from tens of sites across the world. Tracking evolutionary changes in a laboratory setting is a better approach to define the genotype-phenotype relationship.[11,20–23] Integrated analysis of genome resequencing data and gene expression profiling can reveal allelic variation, mutations, and their effects on the regulation of gene expression.[20–22] Therefore, in our study, we used this approach to study the genetic adaptation of DBM to thermal stress.

In the present work, life history traits (lifespan and fecundity) were measured in hot-evolved and control populations of DBM. Transcriptomic and genomic approaches were used to identify the genes harboring allelic variants and changes in expression involved in thermal adaptation. Further, CRISPR/Cas 9 was used to study the function of two ABCG genes in thermal adaptation.

RESULTS

Population fitness of hot-evolved and control strains

The control strain of DBM was maintained on the constant favorable temperature of 26°C. The control strain of DBM (CS) was kept under the elevated temperatures of 27°C for 12 h (dark) and 32°C for 12 h (light) as hot-evolved strain (HS) for one year. The duration of the preadult stage for all generations of the HS strain was significantly shorter than that of the CS strain ($p < 0.001$). The preadult duration of HS30 (CS under elevated environment for 30 generations) was significantly longer than that of HS1 ($p = 0.003$), HS5 (CS under elevated environment for 5 generations) ($p < 0.001$) and HS10 (CS under elevated environment for 10 generations) ($p = 0.010$). The longevity of females did not differ between strains for any generation. The total longevity of CS (15.9 ± 0.1 d) was significantly longer than that of HS for all generations (HS1: 13.4 ± 0.1 d; HS5: 13.2 ± 0.1 d; HS10: 13.5 ± 0.1 d; HS20: 13.5 ± 0.1 d; HS30: 13.6 ± 0.1 d) ($p < 0.001$) (Table S1).

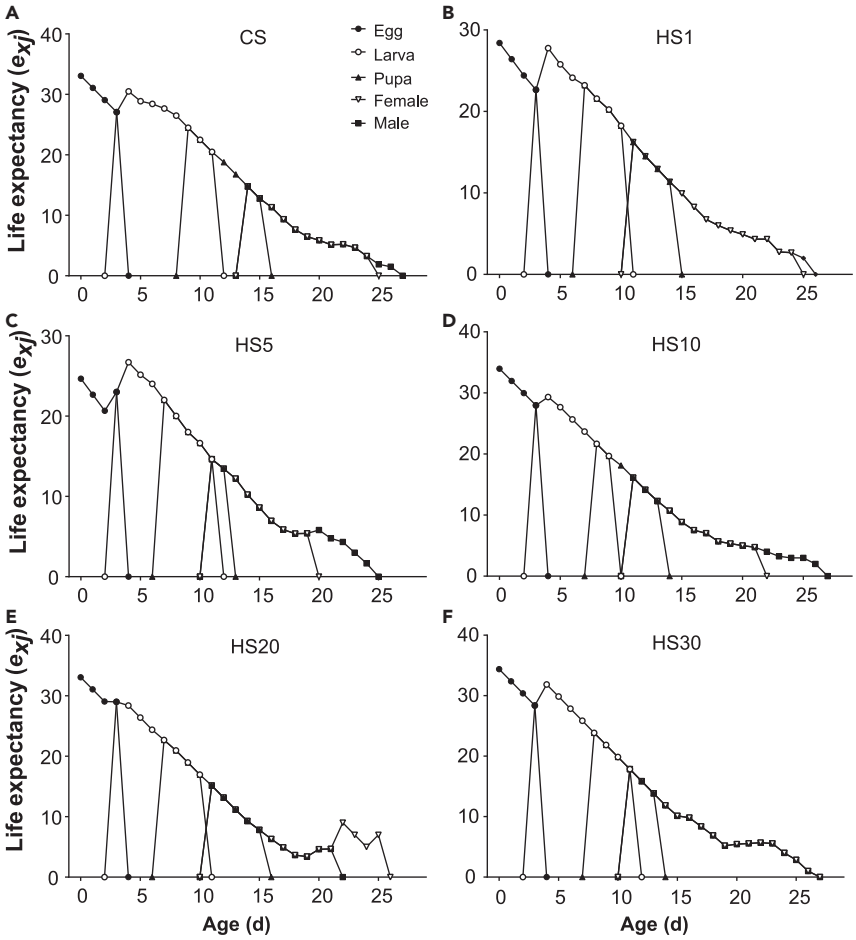

Figure 2. Age-stage specific life expectancy (e_{xj}) of control strain (CS) and hot-evolved strain (HS) of *P. xylostella*

CS (A) represents DBM kept under favorable temperature; and HS1 (B), HS5 (C), HS10 (D), HS20 (E), and HS30 (F) represent the 1st, 5th,10th, 20th, 30th generations of DBM kept under high temperature.

The age-stage survival rate (s_{xj}) represents the probability of a newborn individual surviving to age x and stage j. The survival rate of HS10, HS20 (CS under elevated environment for 20 generations) and HS30 was 0.822 $\pm$ 0.001, 0.856 $\pm$ 0.037 and 0.844 $\pm$ 0.038, respectively, and significantly higher than that of CS, HS1 and HS5 (Figure 1).

The age-stage specific life expectancy (e_{xj}) is the total time that an individual of age x and stage j is expected to survive. The life expectancy of HS1 and HS5 was lower than that of CS. There was no significant difference in this parameter (e_{xj}) between other generations of HS and CS (Figure 2).

Population fitness parameters include intrinsic rate of increase (r), net reproductive rate (R_0), finite rate of increase (λ), and mean generation time (T). The r values of HS10, HS20 and HS30 were significantly higher than that of CS (HS10: $p = 0.002$; HS20: $p < 0.001$; HS30: $p = 0.007$). Only for HS1 was the R_0 value significantly lower than those of CS (HS1: $p = 0.024$). The T values for different generations of HS were all significantly lower than that of CS (HS1: $p < 0.001$; HS5: $p = 0.005$; HS10: $p < 0.001$; HS20: $p < 0.001$; HS30: $p < 0.001$). Except for HS1, the λ values of other generations of HS were all higher than that of CS (HS5: $p = 0.049$; HS10: $p = 0.002$; HS20: $p < 0.001$; HS30: $p = 0.006$) (Table 1).

Responses of HS to high temperatures

The survival rate of CS and HS under high temperatures (39°C, 40°C, 41°C, 42°C, 43°C and 44°C) for 2 h was calculated, respectively. The results showed that both temperature and strain were the critical factors that affecting the survival rate of DBM at extremely high temperatures (Table S2). Compared with CS, the survival rate of HS was significantly increased under high temperatures (39°C, 40°C, 41°C, 42°C, 43°C and 44°C) (Figure 3).

Molecular phenotypes of HS and CS

The transcriptomes of hot-evolved populations (the 33rd generation of HS, HS33) and CS were compared. Of 20,694 genes with reliable expression signals in the two strains, 7,174 were differentially expressed between HS and CS. Of these, 3,414 were up- and 3,760 were downregulated.

Table 1. Population fitness parameters of control strain (CS) and hot-evolved strain (HS) of *P. xylostella*

Parameter	CS	HS1	HS5	HS10	HS20	HS30
r (d^{-1})	0.27 ± 0.01c	0.28 ± 0.01bc	0.30 ± 0.01abc	0.32 ± 0.01ab	0.33 ± 0.01a	0.31 ± 0.01a
R_0	74.92 ± 10.90ab	45.43 ± 7.03c	53.02 ± 7.73b	70.30 ± 9.00ab	83.32 ± 10.06a	83.32 ± 10.06ab
T (d)	15.9 ± 0.1a	13.4 ± 0.1b	13.2 ± 0.1c	13.5 ± 0.1b	13.5 ± 0.1b	13.6 ± 0.1b
λ (d^{-1})	1.31 ± 0.01c	1.33 ± 0.02bc	1.35 ± 0.02ab	1.37 ± 0.01a	1.39 ± 0.01a	1.37 ± 0.01ab

CS represents DBM kept under favorable temperature; and HS5, HS10, HS20 and HS30 represent the 1st, 5th,10th, 20th, 30th generations of DBM kept under high temperature. Different letters indicate significant differences among different treatments ($p < 0.05$).

Contrasting CS to HS, we identified a significant enrichment in several Gene Ontology (GO) categories and Kyoto Encyclopedia of Genes and Genomes (KEGG) pathways. Genes downregulated in HS were enriched for more GO categories than upregulated genes enriched. Upregulated genes exhibited enrichment for several functional categories, including DNA integration, structural constituent of cuticle, cation transport and ion transport (Figure 4A). These genes were also significantly enriched in numerous KEGG signaling pathways, including AMPK, insulin, neurotrophin, PI3K-Aktc and FoxO, as well as other pathways related to oxidative phosphorylation and fatty acid metabolism (Figure 5A). Downregulated genes were enriched for a large number of functions and pathways, such as ribosome and spliceosome (Figures 4B and 5B).

Identification of candidate genes

To identify the candidate genes that underlie population differentiation, we estimated pairwise F_{ST}, π and allele frequency differentiation for all polymorphic SNPs. We identified 13,356 SNPs whose F_{ST} values fell into the top 5% of the F_{ST} distribution ($F_{ST} > 0.178$); and 14,105 SNPs whose π values fell into the top 5% of the distribution ($\pi > 2.378$). In total, 2,156 SNPs were distributed in 445 genes, whose F_{ST} and π values were both in the top 5%. Then, we identified 47,306 SNPs whose allele frequency between CS and HS fell into the top 1% of the distribution (>0.515). Among them, 19,693 SNPs were distributed in 461 genes, whose -$\log_{10}$ (p-value) were >10 (Figure 6). Eventually, 82 genes involved the SNPs that fitted all the above conditions.

Considering the genes with population differentiation and different expressions between CS and HS, we defined 27 genes as candidates selected by high temperature, which included 3 ABCG transporter proteins (*Px008370*, *Px008371* and *Px012058*), mannose transferase (*Px003963*), trehalose transporter (*Px007098*) and rhodopsin (*Px008529*) (Table S3).

SNP mutation and gene expression variation

We sequenced *PxWhite* and *PxABCG* in HS to confirm the mutant SNPs in these candidate genes. We found that 77 SNPs in *PxWhite* of HS were high-frequency mutations, among which, the mutation rates of 44 SNPs were 100% (Figure 7A). Fifty SNPs in *PxABCG* of HS were identified to be high-frequency mutation (Figure 7B).

To verify the function of *PxWhite* and *PxABCG* in mediating adaptation of DBM to extreme temperature, we performed RT-qPCR to profile the gene expression under different temperature regimes using the wild-type strain (WT/CS). At 40°C, 4°C, and −17°C, the expression of *PxWhite* in females was significantly lower than that under 26°C (40°C: $t = 10.973$, $df = 4$, $p < 0.001$; 4°C: $t = 10.142$, $df = 4$, $p = 0.001$; −17°C: $t = 9.945$, $df = 4$, $p = 0.001$). Only at 4°C, *PxWhite* expression of males significantly lower than that at 26°C ($t = 3.128$, $df = 4$, $p = 0.035$). At 40°C, *PxABCG* expression in females was significantly higher than that at 26°C ($t = -3.492$, $df = 4$, $p = 0.025$) (Figure 8).

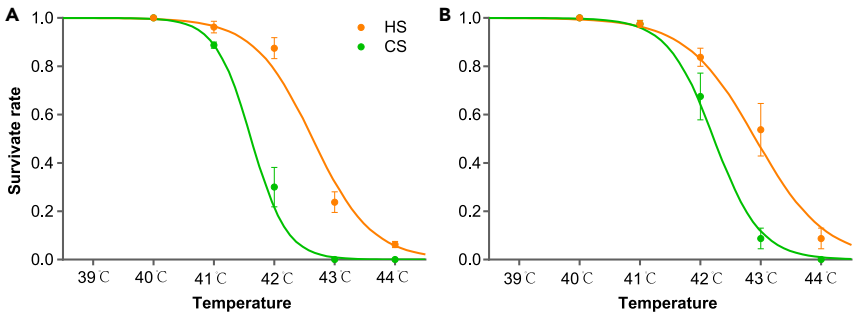

Figure 3. Effect of extremely high temperature on the *P. xylostella* survival rates of CS and HS

Survival rates of *P. xylostella* are presented for females (A) and males (B) after exposure to high temperatures. CS represents DBM kept under favorable temperature; and HS represents DBM kept under high temperature. Survival rates are represented as mean ± SE. Twenty individuals were used for each replicate, with four replicates in each treatment. The curves were generated from the equation $\log[p/(1-p)] = a + b\,T$, where T is temperature (°C).

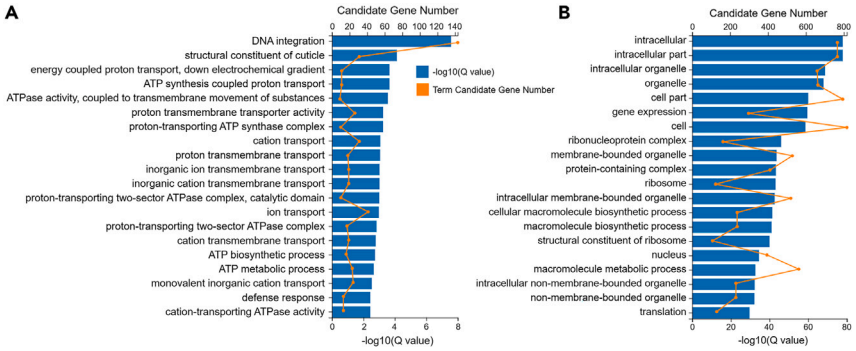

Figure 4. GO ontology classification of DEGs with up- and downregulated patterns

(A) GO enrichment analysis of DEGs with upregulated profiles; and (B) GO enrichment analysis of DEGs with downregulated profiles.

Functional validation of ABCG transporter genes

Using CRISPR/Cas9 genome editing, we successfully knocked out *PxWhite* and *PxABCG* in the WT. A mixture of Cas9 protein and sgRNA of *PxWhite* or *PxABCG* was injected into 216 and 214 eggs, respectively. Among these, 10 and 25 eggs successfully matured to adulthood, respectively. Having been individually crossed with WT, we confirmed site-specific mutagenesis in 30% (3/10) and 24% (6/25) of G0 moths,

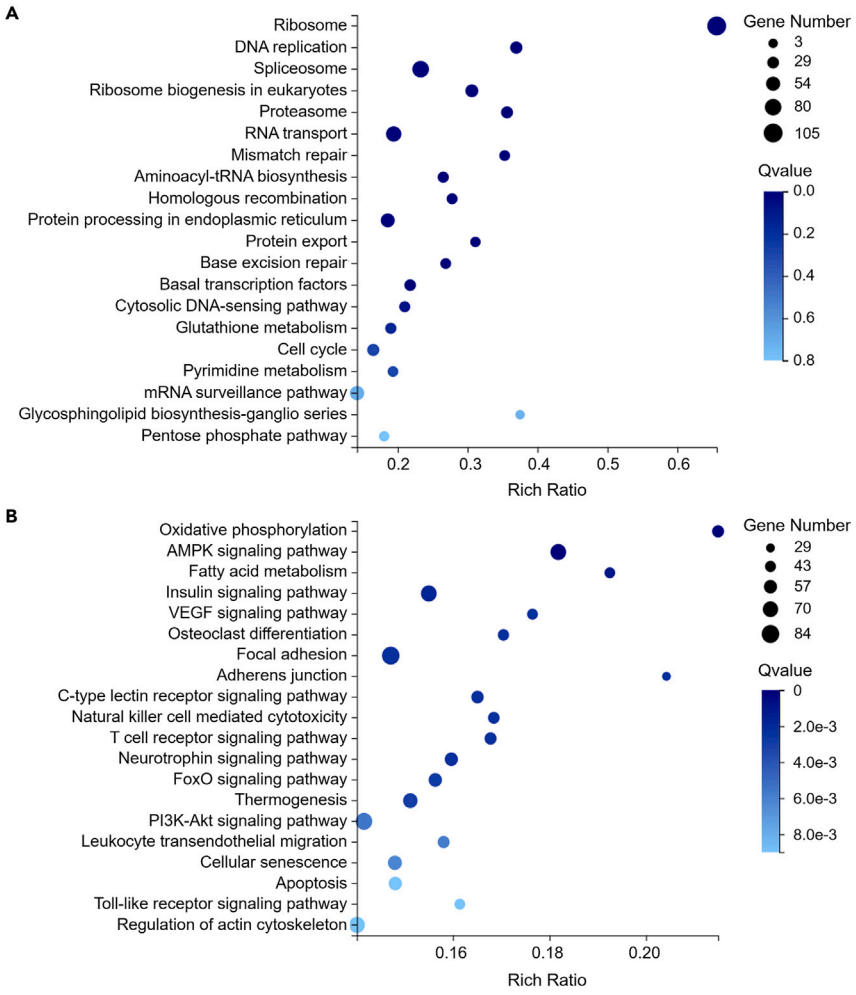

Figure 5. KEGG (Kyoto Encyclopedia of Genes and Genomes) pathway enrichment analysis of DEGs with up- and downregulated patterns

(A) KEGG pathway enrichment analysis of DEGs with upregulated profiles; and (B) KEGG pathway enrichment analysis of DEGs with downregulated profiles.

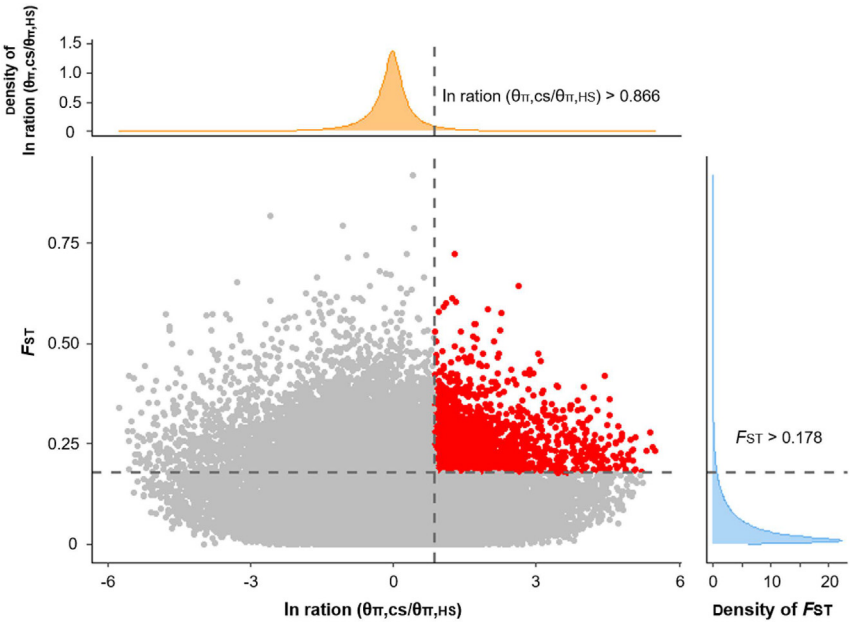

Figure 6. Distribution of ln ratio ($\theta_{\pi,\ CS}/\theta_{\pi,\ HS}$) and F_{ST}

Red dots represent windows fitting the selected regions requirement (corresponding to ratio ($\theta_{\pi,\ CS}/\theta_{\pi,\ HS}$) > 0.866, F_{ST} > 0.178).

respectively. After mutation screening, one homozygous mutant strain with a 1-bp insertion in *PxWhite* exon 3 and one homozygous mutant strain with a 4-bp deletion in *PxABCG* exon 4 were generated (Figure 9).

We examined the difference in the percentage of larvae that could develop into pupae after heat shock between the strain of the wild-type and the *PxWhite* mutant or *PxABCG* mutant. At 42°C or 43°C for 2h, we found that fewer fourth instar larvae of the *PxWhite*-MU and *PxABCG*-MU strains developed into pupae than those of CS (Figure 10A). We then examined the difference in survival rate between the CS, *PxWhite*-MU, and *PxABCG*-MU adults under high temperatures (40°C, 41°C, 42°C and 43°C). Compared with CS, survival of the *PxWhite*-MU and *PxABCG*-MU were significantly reduced under high temperatures (Tables S4 and S5; Figures 10B and 10C).

To assess the impact of *PxABCG* and *PxWhite* mutations on cuticle permeability, we employed Eosin Y staining. The resulting image (Figure 11) provides a clear visual representation of the differential permeability patterns. In wild-type (WT) larvae, most body surfaces were impermeable to Eosin Y, with staining restricted to the head, the third abdominal leg, and the fifth anal leg. In contrast, larvae of both mutant strains exhibited a compromised surface barrier, allowing Eosin Y to penetrate the entire body, as evidenced by the extensive staining observed in PxWhite-MU and PxABCG-MU larvae (Figure 11).

DISCUSSION

Temperature is a major factor influencing the behavior, physiology, and genetics of ectotherms. Our experimental DBM populations, pre-adapted to elevated temperature, showed highly significant differences in gene expression and SNP mutants. A number of genes were identified that are involved in the thermal adaptation of this global pest. Using CRISPR/Cas9 genome editing, two ABCG genes were shown to be involved in the adaptation of DBM to elevated temperatures.

The fitness parameters of DBM under thermal stress were monitored for 30 generations and the intrinsic rate of increase recovered after five generations and was not significantly lower than that of the control strain. The finite rate of increase (λ) of HS was higher than that of CS. After 10 generations of acclimation under thermal environment, the net reproductive rate (R_0) was obviously increased. Our observations indicate that DBM in fitness are able to adapt to substantially higher temperatures within 5–10 generations. In addition, heat-adapted DBM have a higher thermal tolerance than the control DBM.

We then combined transcriptomic and genomic approaches to explore the genetic adaptation of DBM to the thermal environment. After 33 generations of high temperature acclimation, the DBM populations displayed highly significant differences in gene expression. Most previous studies of thermal plasticity in insects have focused on short-term heat shock, corresponding to a short exposure to high temperature for tens of minutes or hours.[24–26] However, the genetic adaptation in nature usually takes a relatively long time. Studies of long-term acclimation have mainly focused on the model organism *D. melanogaster*, with several cases of environmental temperature affecting gene expression profiles[11] and protein profiles.[27,28] Mallard et al.[11] show that the metabolism of *D. melanogaster* is rewritten after 60 generations in a hot environment, involving two key genes, *Sestrin* and *SNF4Ay*, implicating AMPK. Here, we also found that the AMPK signaling pathway was enriched in upregulated genes in hot-evolved populations.

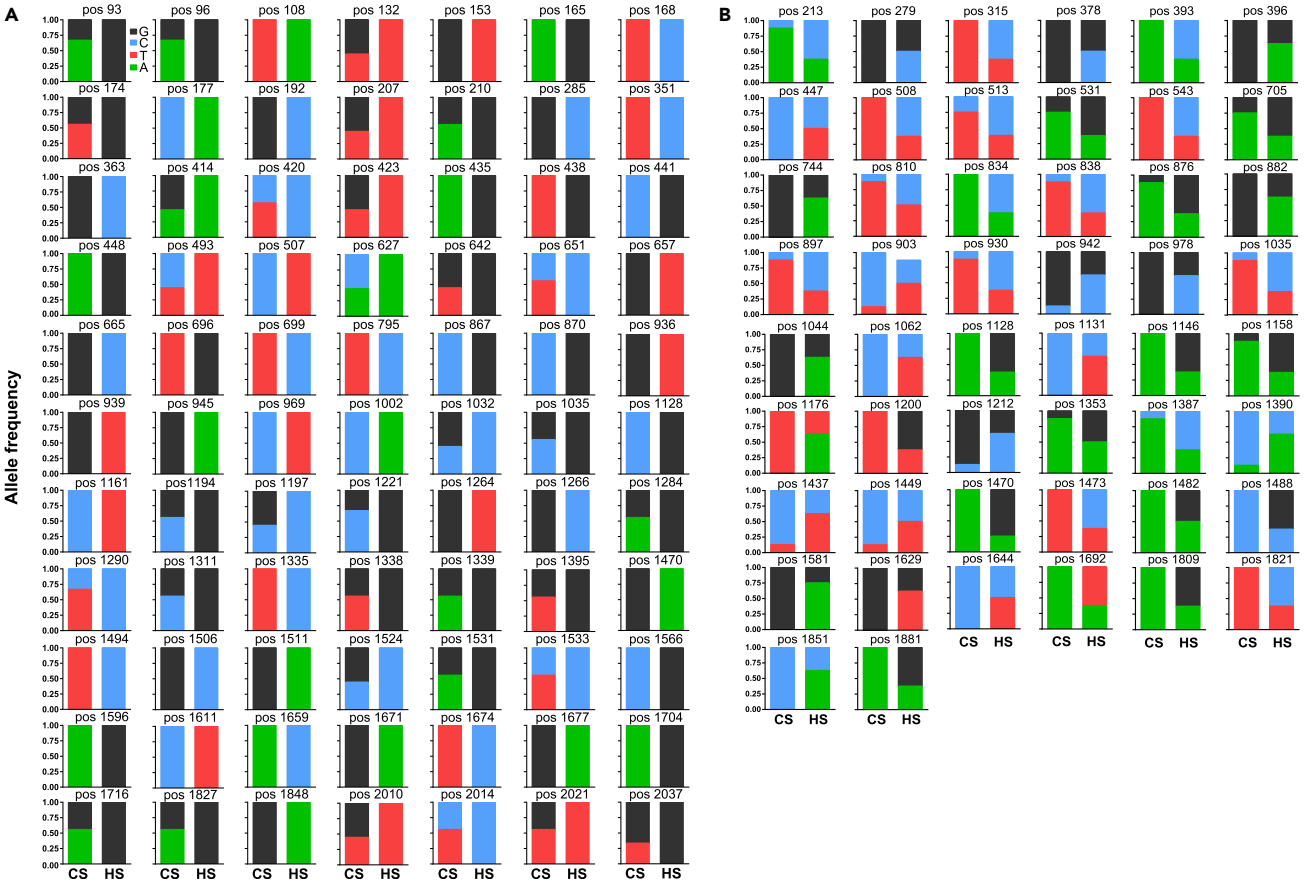

Figure 7. The mutant SNPs of *PxWhite* and *PxABCG* in CS and HS DBM

(A) The allele frequency of mutant SNPs of *PxWhite*; and (B) The allele frequency of mutant SNPs of *PxABCG*. pos indicates position of SNPs in gene. CS represents DBM kept under favorable temperature; and HS represents DBM kept under high temperature. The colors represent: black: G base; blue: C base; red: T base; green: A base.

In the present study, we focused on the change in gene expression resulting from the genetic change. Therefore, a common garden experiment was performed to determine the change in gene expression between CS and HS. We then combined the transcriptomic and genomic data to identify the genes that changed at both RNA and DNA levels. Twenty-seven genes were identified as being involved in the thermal adaptation of DBM. These genes are predicted to cover a wide range of functions. Among them, some genes were previously documented with regulating the response of species to temperature. For example, the long-chain fatty acid-CoA ligase 1 (*Px017708*) was involved in catalyzing the conversion of long-chain fatty acids to active acyl-CoA and synthesis of cellular lipids, which plays an important role in the response of animals to cold.[29,30] Trehalose transporter (*Px007098*) was responsible for releasing of trehalose from the insect's fat body into the hemolymph and transferring it to other tissues to balance the trehalose content in the hemolymph.[31] Trehalose could help insects resist temperature stress.[32–34] The expression of trehalose transporter in *Anopheles gambiae* is upregulated at high temperatures and after RNAi of this gene, the thermal tolerance of *A. gambiae* is reduced.[33]

Three of the previously documented genes were members of the ABC transporter subfamily G (http://59.79.254.1/DBM/index.php). In our study, we have only confirmed the functions of two ABCG transporter genes (*Px008371/PxWhite* and *Px012058/PxABCG*), as we could not establish the strain of the *Px008370* mutant. The gene expressions of *PxWhite* and *PxABCG* under high temperature (40°C) were significantly different from that under favorable temperature for DBM (26°C). Furthermore, the SNP mutation of these two genes was higher in the hot-evolved populations. We then used the CRISPR/Cas 9 technique to generate *PxWhite* knockout and *PxABCG* knockout DBM strains. The thermal tolerance of DBM was reduced after *PxWhite* and *PxABCG* knockout. In *Drosophila*, the white gene is involved in the vesicular transepithelial transport of guanosine 3′-5′ cyclic monophosphate, which indirectly affects the lipid transport.[35] The white gene mutants in *D. melanogaster* have defects in olfactory learning and cholesterol homeostasis, potentially due to alterations in lipid composition and/or distribution.[36] TcABCG-4C of *Tribolium castaneum* acts as a transporter of cuticular lipids deposited in the outer epicuticular layer to prevent water loss.[37] The epicuticular lipid layer of insects plays a fundamental role in insect fitness and acts as a selective barrier against water loss, thus preventing lethal desiccation.[38–41] However, under extremely high temperatures, water loss is an important cause of insect death.[42] In our study, we also speculated that *PxWhite* and *PxABCG* might be involved in thermal adaptation

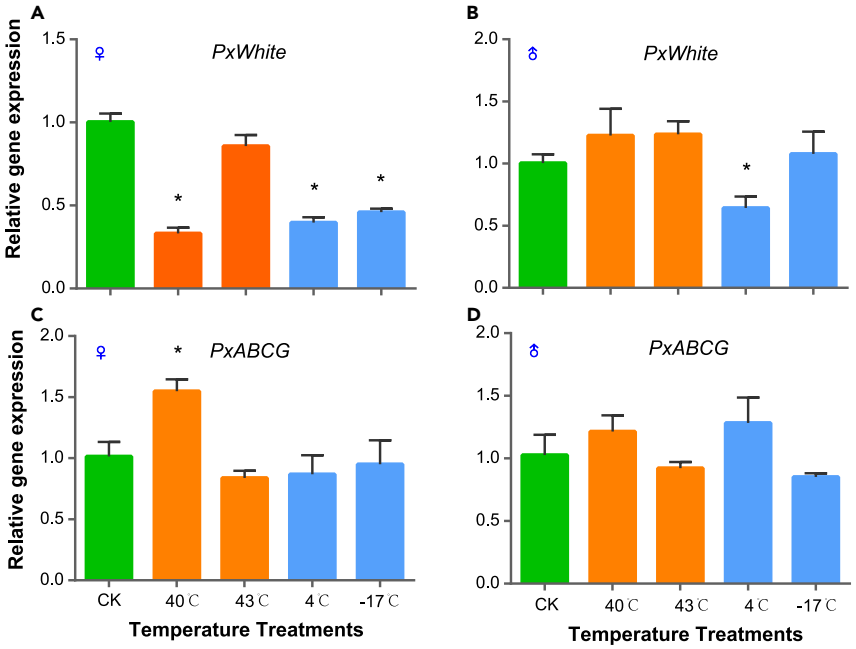

Figure 8. Effect of extreme temperatures on the relative expression level of the *PxWhite* and *PxABCG* genes in the wild-type DBM strain (WT)

(A) Expression level of *PxWhite* in females.

(B) Expression level of *PxWhite* in males.

(C) Expression level of *PxABCG* in females.

(D) Expression level of *PxABCG* in males. Temperature treatments included two high-temperatures treatments: (1) 40°C for 30 min, (2) 43°C for 30 min; and two low-temperature treatments: (1) 4°C for 30 min, and (2) −17°C for 30 min. Expression of *PxWhite/PxABCG* at 26°C was arranged as control with a relative expression value = 1. Error bars represent the standard error of the mean. Expression of *PxWhite/PxABCG* in each treatment was statistically compared with control using independent t-test. * denotes significant difference between control and each of the treatments (t-test, $p < 0.05$).

by altering the cuticle permeability of DBM. Therefore, we used Eosin Y staining to verify that *PxWhite* and *PxABCG* mutants improved the cuticle permeability of DBM, which could maintain the water balance of insect body. Further research is needed to explore how *PxWhite* and *PxABCG* to alter the cuticle permeability of DBM.

This is the first report suggesting that ABCG subfamily genes are involved in thermal tolerance and adaptation of insects. Currently, studies on the ABCG transporter of DBM are related to eye color and Bt resistance. The white gene is required for normal eye pigmentation in many insects,[43,44] including DBM. In our study, we observed the white-eyed DBM in the *PxWhite* mutant strain. *PxWhite* is also involved in Cry1Ac resistance in DBM.[45] Several ABCG transporters have been shown to be involved in lipid transport and cholesterol homeostasis.[46–49]

The absence of overlap between the candidate genes identified in this study and those from our previous landscape genomics analysis of DBM's genomic variation and climate variables[19] can be attributed to the distinct selection pressures experienced by the respective populations. In the previous study, DBM samples were collected from the wild, where they were subjected to a multitude of environmental factors, while the laboratory-developed population in the current study was exposed solely to temperature-based selection. This difference in selective environments likely accounts for the divergent sets of candidate genes identified in the two studies.

Limitations of the study

Rapid phenotypic evolution is common in nature and observed in evolution experiments. It can be attributed to either subtle frequency changes in genetic polymorphisms across many loci[50–52] or to a few loci or genes with large effects.[53] In our laboratory evolution, we observed extensive frequency changes in genetic variants, suggesting that both polygenic and oligogenic factors may have driven rapid evolution. Further functional verification of the candidate genes identified in our study will provide more critical information insights into the genetic mechanisms underlying rapid evolution. Allelic replacement using CRISPR/Cas9 technology enables the investigation of the relationship between SNP mutations and thermal adaptation. Thus, further work is needed to understand the role of SNP mutations in candidate genes in the adaptation of DBM to the thermal environment.

Conclusions

In the face of global warming, it is important to understand how insect pests respond and adapt to increased temperatures in order to predict future risks and identify potential, novel targets for insecticidal or genetic control. We integrated analysis of changes in SNP and gene expression levels in laboratory-evolved populations to identify the genes involved in the thermal adaptation of DBM. *PxWhite* and *PxABCG*

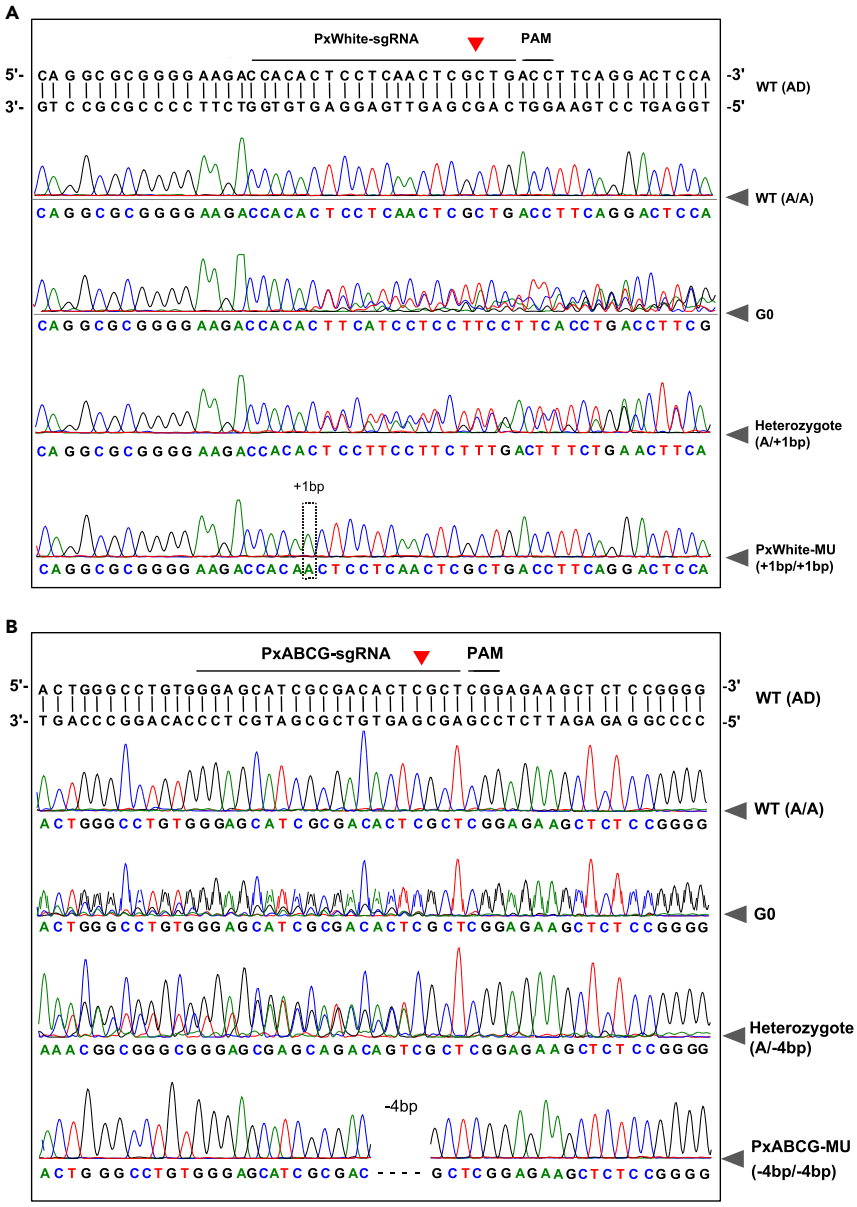

Figure 9. Mutagenesis of *PxWhite* and *PxACBG* induced by CRISPR/Cas9

Representative sequencing trace of the PCR fragment from mutated G0 adults with multi-peaks at the cleavage site and representative sequence of the diverse indel mutations flanking the sgRNA target sites of *PxWhite* (A) and *PxABCG* (B) in the G0 individuals. (A) The base in the dotted box denotes the insertion mutation kept establishing the *PxWhite* mutant strain. (B) The dotted line denotes the deletion mutation kept establishing the *PxABCG* mutant strain.

regulated DBM susceptibility to high temperature by altering cuticle permeability. This suggests that ABCG transporter genes play an important role in the thermal adaptation of DBM and potentially other insect pests for which new control methods are needed to combat insecticide resistance and prevent crop losses.

STAR★METHODS

Detailed methods are provided in the online version of this paper and include the following:

- KEY RESOURCES TABLE
- RESOURCE AVAILABILITY
  - Lead contact
  - Materials availability

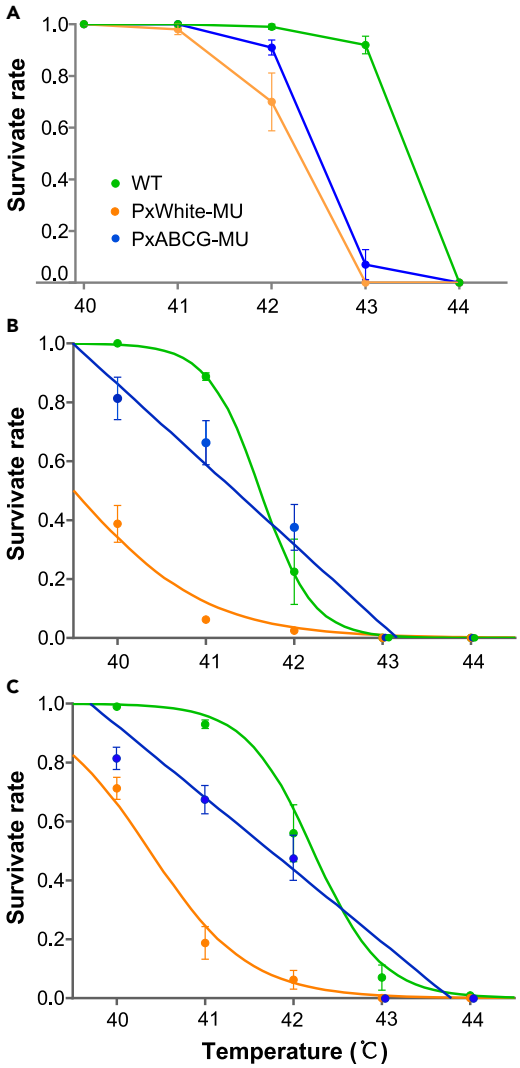

Figure 10. Effect of extremely high temperature on survival rates of the wild-type, *PxWhite*-deficient and *PxABCG*-deficient diamondback moth

(A) The percentage of fourth-instar larvae of DBM developed into pupae after exposure to high temperatures. Survival rates of DBM are presented for females (B) and males (C) after exposure to high temperatures. Survival rates are represented as mean ± SE. Twenty individuals were used for each replicate, with four replicates in each treatment. The curves were generated from the equation: $\log[p/(1-p)] = a + b\,T$ where T is temperature (°C). The significant test was in the Tables S4 and S5.

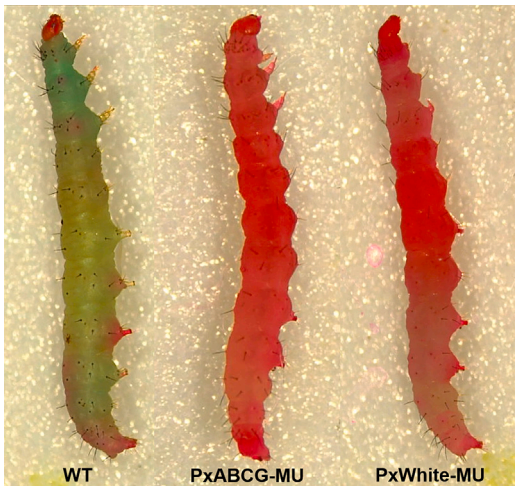

Figure 11. The larvae of WT, *PxABG*-MU and *PxWhite*-MU were stained with Eosin Y

SUPPLEMENTAL INFORMATION

Supplemental information can be found online at https://doi.org/10.1016/j.isci.2024.109242.

ACKNOWLEDGMENTS

The work was supported by the National Natural Science Foundation of China (32202312, 31972271), the Hainan Major Science and Technology Project (ZDKJ202002), the Natural Science Foundation for Distinguished Young Scholars of Fujian Province (2022J06013), the project of Fujian Academy of Agricultural Sciences (GJYS202303), the Fujian Science and Technology Project (2022L3087), the Fujian Agriculture and Forestry University Science and Technology Innovation Fund Project (CXZX2019001G, CXZX2017206), and the Outstanding Young Scientific Research Talents Program of Fujian Agriculture and Forestry University (xjq201905). This work was also supported by the high-performance computing platform of YZBSTCACC.

AUTHOR CONTRIBUTIONS

Conceptualization, S.Y. and Y.C.; Methodology, S.Y., G.L., H.Z., and Y.C.; Investigation, S.Y., G.L., H.Z., J.L., S.C., J.H., and Y.C.; Writing - Original Draft: S.Y. and Y.C.; Writing – Review and Editing, S.Y., Y.C., L.V., G.M.G., and M.Y.; Visualization, G.L. and Y.C.; Supervision, Y.C. and M.Y.; Funding Acquisition, Y.C. and M.Y.

DECLARATION OF INTERESTS

The authors declare no competing interests.

Received: July 3, 2023
Revised: October 16, 2023
Accepted: February 12, 2024
Published: February 15, 2024

REFERENCES

1. Harvey, J.A., Heinen, R., Gols, R., and Thakur, M.P. (2020). Climate change-mediated temperature extremes and insects: From outbreaks to breakdowns. Glob. Chang. Biol. *26*, 6685–6701.
2. Colinet, H., Sinclair, B.J., Vernon, P., and Renault, D. (2015). Insects in fluctuating thermal environments. Annu. Rev. Entomol. *60*, 123–140.
3. Field, C.B., Barros, V.R., Dokken, D.J., Mastrandrea, M.D., and Mach, K.J. (2014). Climate Change 2014: Impacts, Adaptation and Vulnerability (Cambridge University Press).
4. González-Tokman, D., Córdoba-Aguilar, A., Dáttilo, W., Lira-Noriega, A., Sánchez-Guillén, R.A., and Villalobos, F. (2020). Insect responses to heat: physiological mechanisms, evolution and ecological implications in a warming world. Biol. Rev. *95*, 802–821.
5. Huey, R.B., Kearney, M.R., Krockenberger, A., Holtum, J.A.M., Jess, M., and Williams, S.E. (2012). Predicting organismal vulnerability to climate warming: roles of behaviour, physiology and adaptation. Phil. Trans. R. Soc. B. *367*, 1665–1679.
6. Hoffmann, A.A. (2010). Physiological climatic limits in *Drosophila*: patterns and implications. J. Exp. Biol. *213*, 870–880.
7. Somero, G.N. (2010). The physiology of climate change: how potentials for acclimatization and genetic adaptation will determine 'winners' and 'losers'. J. Exp. Biol. *213*, 912–920.
8. Sunday, J.M., Bates, A.E., Kearney, M.R., Colwell, R.K., Dulvy, N.K., Longino, J.T., and Huey, R.B. (2014). Thermal-safety margins and the necessity of thermoregulatory behavior across latitude and elevation. Proc. Natl. Acad. Sci. USA *111*, 5610–5615.
9. Esperk, T., Kjaersgaard, A., Walters, R.J., Berger, D., and Blanckenhorn, W.U. (2016). Plastic and evolutionary responses to heat stress in a temperate dung fly: negative correlation between basal and induced heat tolerance? J. Evol. Biol. *29*, 900–915.

10. Lafuente, E., and Beldade, P. (2019). Genomics of developmental plasticity in animals. Front. Genet. *10*, 720.
11. Mallard, F., Nolte, V., Tobler, R., Kapun, M., and Schlötterer, C. (2018). A simple genetic basis of adaptation to a novel thermal environment results in complex metabolic rewiring in *Drosophila*. Genome Biol. *19*, 119.
12. Liu, Y., Su, H., Li, R., Li, X., Xu, Y., Dai, X., Zhou, Y., and Wang, H. (2017). Comparative transcriptome analysis of *Glyphodes pyloalis* Walker (Lepidoptera: Pyralidae) reveals novel insights into heat stress tolerance in insects. BMC Genom. *18*, 974.
13. Li, H., Zhao, X., Qiao, H., He, X., Tan, J., and Hao, D. (2019). Comparative transcriptome analysis of the heat stress response in *Monochamus alternatus* Hope (Coleoptera: Cerambycidae). Front. Physiol. *10*, 1568.
14. Dewitt, T.J., and Scheiner, S.M. (2004). Phenotypic Plasticity: Functional and Conceptual Approaches (Oxford University Press).
15. Wang, X.R., Wang, C., Ban, F.X., Zhu, D.T., Liu, S.S., and Wang, X.W. (2019). Genome-wide identification and characterization of HSP gene superfamily in whitefly (*Bemisia tabaci*) and expression profiling analysis under temperature stress. Insect Sci. *26*, 44–57.
16. Sørensen, J.G., Giribets, M.P., Tarrío, R., Rodríguez-Trelles, F., Schou, M.F., and Loeschcke, V. (2019). Expression of thermal tolerance genes in two *Drosophila* species with different acclimation capacities. J. Therm. Biol. *84*, 200–207.
17. Rodrigues, Y.K., and Beldade, P. (2020). Thermal plasticity in insects' response to climate change and to multifactorial environments. Front. Ecol. Evol. *8*, 271.
18. You, M., Ke, F., You, S., Wu, Z., Liu, Q., He, W., Baxter, S.W., Yuchi, Z., Vasseur, L., Gurr, G.M., et al. (2020). Variation among 532 genomes unveils the origin and evolutionary history of a global insect herbivore. Nat. Commun. *11*, 2321.
19. Chen, Y., Liu, Z., Régnière, J., Vasseur, L., Lin, J., Huang, S., Ke, F., Chen, S., Li, J., Huang, J., et al. (2021). Large-scale genome-wide study reveals climate adaptive variability in a cosmopolitan pest. Nat. Commun. *12*, 7206.
20. Portnoy, V.A., Bezdan, D., and Zengler, K. (2011). Adaptive laboratory evolution–harnessing the power of biology for metabolic engineering. Curr. Opin. Biotechnol. *22*, 590–594.
21. Conrad, T.M., Lewis, N.E., and Palsson, B.Ø. (2011). Microbial laboratory evolution in the era of genome-scale science. Mol. Syst. Biol. *7*, 509.
22. Hindré, T., Knibbe, C., Beslon, G., and Schneider, D. (2012). New insights into bacterial adaptation through *in vivo* and in silico experimental evolution. Nat. Rev. Microbiol. *10*, 352–365.
23. Latif, H., Sahin, M., Tarasova, J., Tarasova, Y., Portnoy, V.A., Nogales, J., and Zengler, K. (2015). Adaptive evolution of *Thermotoga maritima* reveals plasticity of the ABC Transporter network. Appl. Environ. Microbiol. *81*, 5477–5485.
24. van Heerwaarden, B., Kellermann, V., Sgrò, C.M., and Williams, C. (2016). Limited scope for plasticity to increase upper thermal limits. Funct. Ecol. *30*, 1947–1956.
25. Kellermann, V., van Heerwaarden, B., and Sgrò, C.M. (2017). How important is thermal history? Evidence for lasting effects of developmental temperature on upper thermal limits in *Drosophila melanogaster*. Proc. Biol. Sci. *284*, 20170447.
26. Ma, C.S., Ma, G., and Pincebourde, S. (2021). Survive a warming climate: Insect responses to extreme high temperatures. Annu. Rev. Entomol. *66*, 163–184.
27. Colinet, H., Overgaard, J., Com, E., and Sørensen, J.G. (2013). Proteomic profiling of thermal acclimation in *Drosophila melanogaster*. Insect Biochem. Mol. Biol. *43*, 352–365.
28. Kristensen, T.N., Kjeldal, H., Schou, M.F., and Nielsen, J.L. (2016). Proteomic data reveal a physiological basis for costs and benefits associated with thermal acclimation. J. Exp. Biol. *219*, 969–976.
29. Ellis, J.M., Li, L.O., Wu, P.C., Koves, T.R., Ilkayeva, O., Stevens, R.D., Watkins, S.M., Muoio, D.M., and Coleman, R.A. (2010). Adipose acyl-CoA synthetase-1 directs fatty acids toward beta-oxidation and is required for cold thermogenesis. Cell Metab. *12*, 53–64.
30. Nguyen, K.D., Qiu, Y., Cui, X., Goh, Y.P.S., Mwangi, J., David, T., Mukundan, L., Brombacher, F., Locksley, R.M., and Chawla, A. (2011). Alternatively activated macrophages produce catecholamines to sustain adaptive thermogenesis. Nature *480*, 104–108.
31. Kanamori, Y., Saito, A., Hagiwara-Komoda, Y., Tanaka, D., Mitsumasu, K., Kikuta, S., Watanabe, M., Cornette, R., Kikawada, T., and Okuda, T. (2010). The trehalose transporter 1 gene sequence is conserved in insects and encodes proteins with different kinetic properties involved in trehalose import into peripheral tissues. Insect Biochem. Mol. Biol. *40*, 30–37.
32. Benoit, J.B., Lopez-Martinez, G., Elnitsky, M.A., Lee, R.E., Jr., and Denlinger, D.L. (2009). Dehydration-induced cross tolerance of *Belgica antarctica* larvae to cold and heat is facilitated by trehalose accumulation. Comp. Biochem. Physiol. Mol. Integr. Physiol. *152*, 518–523.
33. Liu, K., Dong, Y., Huang, Y., Rasgon, J.L., and Agre, P. (2013). Impact of trehalose transporter knockdown on Anopheles gambiae stress adaptation and susceptibility to *Plasmodium falciparum* infection. Proc. Natl. Acad. Sci. USA *110*, 17504–17509.
34. Karpova, E.K., Eremina, M.A., Pirozhkova, D.S., and Gruntenko, N.E. (2019). Stress-related hormones affect carbohydrate metabolism in *Drosophila* females. Arch. Insect Biochem. Physiol. *101*, e21540.
35. Evans, E.W., Carlile, N.R., Innes, M.B., and Pitigala, N. (2013). Warm springs reduce parasitism of the cereal leaf beetle through phenological mismatch. J. Appl. Entomol. *137*, 383–391.
36. Myers, J.L., Porter, M., Narwold, N., Bhat, K., Dauwalder, B., and Roman, G. (2021). Mutants of the white ABCG Transporter in *Drosophila melanogaster* Have deficient olfactory learning and cholesterol Homeostasis. Int. J. Mol. Sci. *22*, 12967.
37. Broehan, G., Kroeger, T., Lorenzen, M., and Merzendorfer, H. (2013). Functional analysis of the ATP-binding cassette (ABC) transporter gene family of *Tribolium castaneum*. BMC Genom. *14*, 6.
38. Wigglesworth, V.B. (1945). Transpiration through the cuticle of insects. J. Exp. Biol. *21*, 97–114.
39. Wigglesworth, V.B. (1985). Sclerotin and lipid in the waterproofing of the insect cuticle. Tissue Cell *17*, 227–248.
40. Juárez, M.P., and Fernández, G.C. (2007). Cuticular hydrocarbons of triatomines. Comp. Biochem. Physiol. Mol. Integr. Physiol. *147*, 711–730.
41. Hadley, N.F. (1982). Cuticle ultrastructure with respect to the lipid waterproofing barrier. J. Exp. Zool. *222*, 239–248.
42. Chown, S.L., Sørensen, J.G., and Terblanche, J.S. (2011). Water loss in insects: an environmental change perspective. J. Insect Physiol. *57*, 1070–1084.
43. Mackenzie, S.M., Howells, A.J., Cox, G.B., and Ewart, G.D. (2000). Sub-cellular localisation of the white/scarlet ABC transporter to pigment granule membranes within the compound eye of *Drosophila melanogaster*. Genetica *108*, 239–252.
44. Yan, Y., Ziemek, J., and Schetelig, M.F. (2020). CRISPR/Cas9 mediated disruption of the white gene leads to pigmentation deficiency and copulation failure in *Drosophila suzukii*. J. Insect Physiol. *126*, 104091.
45. Guo, Z., Kang, S., Zhu, X., Wu, Q., Wang, S., Xie, W., and Zhang, Y. (2015). The midgut cadherin-like gene is not associated with resistance to Bacillus thuringiensis toxin Cry1Ac in *Plutella xylostella* (L.). J. Invertebr. Pathol. *126*, 21–30.
46. Kerr, I.D., Haider, A.J., and Gelissen, I.C. (2011). The ABCG family of membrane-associated transporters: you don't have to be big to be mighty. Br. J. Pharmacol. *164*, 1767–1779.
47. Dermauw, W., and Van Leeuwen, T. (2014). The ABC gene family in arthropods: comparative genomics and role in insecticide transport and resistance. Insect Biochem. Mol. Biol. *45*, 89–110.
48. Tarr, P.T., Tarling, E.J., Bojanic, D.D., Edwards, P.A., and Baldán, A. (2009). Emerging new paradigms for ABCG transporters. Biochim. Biophys. Acta *1791*, 584–593.
49. Nagao, K., Juni, N., and Umeda, M. (2015). Membrane lipid transporters in Drosophila melanogaster in bioactive lipid mediators. In Bioactive Lipid Mediators, T. Yokomizo, ed., pp. 165–180.
50. Wellenreuther, M., and Hansson, B. (2016). Detecting polygenic evolution: problems, pitfalls, and promises. TIG (Trends Genet.) *32*, 155–164.
51. Pritchard, J.K., and Di Rienzo, A. (2010). Adaptation–not by sweeps alone. Nat. Rev. Genet. *11*, 665–667.
52. Rockman, M.V. (2012). The QTN program and the alleles that matter for evolution: all that's gold does not glitter. Evolution *66*, 1–17.
53. Messer, P.W., Ellner, S.P., and Hairston, N.G. (2016). Can population genetics adapt to rapid evolution? Trends Genet. *32*, 408–418.
54. Chi, H., You, M., Atlıhan, R., Smith, C.L., Kavousi, A., Özgökçe, M.S., Güncan, A., Tuan, S.J., Fu, J.W., Xu, Y.Y., et al. (2020). Age-Stage, two-sex life table: an introduction to theory, data analysis, and application. Entomol. Gen. *40*, 103–124.
55. Chen, Y., Chen, Y., Shi, C., Huang, Z., Zhang, Y., Li, S., Li, Y., Ye, J., Yu, C., Li, Z., et al. (2018). SOAPnuke: a MapReduce acceleration-supported software for integrated quality control and preprocessing of high-throughput sequencing data. GigaScience *7*, 1–6.
56. Li, H., and Durbin, R. (2009). Fast and accurate short read alignment with Burrows-Wheeler transform. Bioinformatics *25*, 1754–1760.
57. Li, H., Handsaker, B., Wysoker, A., Fennell, T., Ruan, J., Homer, N., Marth, G., Abecasis, G.,

and Durbin, R.; 1000 Genome Project Data Processing Subgroup (2009). The sequence alignment/map format and SAMtools. Bioinformatics *25*, 2078–2079.

58. Kofler, R., Orozco-terWengel, P., De Maio, N., Pandey, R.V., Nolte, V., Futschik, A., Kosiol, C., and Schlötterer, C. (2011). PoPoolation: a toolbox for population genetic analysis of next generation sequencing data from pooled individuals. PLoS One *6*, e15925.
59. Kofler, R., Pandey, R.V., and Schlötterer, C. (2011). PoPoolation2: identifying differentiation between populations using sequencing of pooled DNA samples (Pool-Seq). Bioinformatics *27*, 3435–3436.
60. Langmead, B., and Salzberg, S.L. (2012). Fast gapped-read alignment with Bowtie 2. Nat. Methods *9*, 357–359.
61. Li, B., and Dewey, C.N. (2011). RSEM: accurate transcript quantification from RNA-Seq data with or without a reference genome. BMC Bioinf. *12*, 323.
62. Love, M.I., Huber, W., and Anders, S. (2014). Moderated estimation of fold change and dispersion for RNA-seq data with DESeq2. Genome Biol. *15*, 550.
63. Liu, S.S., Chen, F.Z., and Zalucki, M.P. (2002). Development and survival of the diamondback moth (Lepidoptera: Plutellidae) at constant and alternating temperatures. Environ. Entomol. *31*, 221–231.
64. Chi, H., and Liu, H. (1985). Two new methods for the study of insect population ecology. Bull. Inst. Zool. Acad. Sin. (Taipei) *24*, 225–240.
65. Chi, H. (1988). Life-table analysis incorporating both sexes and variable development rates among individuals. Environ. Entomol. *17*, 26–34.
66. Futschik, A., and Schlötterer, C. (2010). The next generation of molecular markers from massively parallel sequencing of pooled DNA samples. Genetics *186*, 207–218.
67. Livak, K.J., and Schmittgen, T.D. (2001). Analysis of relative gene expression data using real-time quantitative PCR and the 2(-Delta Delta C(T)) Method. Methods *25*, 402–408.

STAR★METHODS

KEY RESOURCES TABLE

REAGENT or RESOURCE	SOURCE	IDENTIFIER
Critical commercial assays		
DNeasy Blood and Tissue Kit	Qiagen	Cat#69504
Eastep® Super Total RNA Extraction kit	Promega	Cat#LS1040
GoScriptTM Reverse Transcription System	Promega	Cat#A5001
Phanta Max Super-Fidelity DNA Polymerase	Vazyme	Cat#P505-d1
Gel Extraction Kit	Omega	Cat#D2500-01
SYBR Green Supermix	Promega	Cat#A6001
HiScribe™ T7 Quick High Yield RNA Synthesis Kit	New England Biolabs	Cat#E2040S
TiANamp Genomic DNA Kit	TIANGEN	Cat#DP304-02
0.5% Eosin Y	Scientific Phygene	Cat#PH0720
Deposited data		
Whole genome resequencing data	This paper	CRA014483, https://ngdc.cncb.ac.cn/gsa
Transcriptome data	This paper	CRA014495,https://ngdc.cncb.ac.cn/gsa
Experimental models: Organisms/strains		
WT/CS	Storage in lab	N/A
HS	Storage in lab	N/A
Pxwhite-MU	Storage in lab	N/A
PxABCG-MU	Storage in lab	N/A
Oligonucleotides		
Primer for PCR in SNP mutant detecting: PxWhite: forward: ATGACGGCGGGAAATGAGGAGCAGGAGC; reverse: TTATTTCGCCCTGCGCGTCCTCAGGACCAG	This paper	N/A
Primer for PCR in SNP mutant detecting: PxABCG: forward: AGTGCGTCGTGCTATAGTGGG; reverse: AGTGCGTCGTGCTATAGTGGG	This paper	N/A
Primer for RT-qPCR: PxWhite: forward: AGAAGTCATATCGGAGTTG; reverse: GTATAACATTCTGTGCCATAA	This paper	N/A
Primer for RT-qPCR: PxABCG: forward: CAAGTTGGGTAGTGAGCTCGG; reverse: ATGGAGAGCCGCTTGTACTGC	This paper	N/A
Primer for obtaining the templates for *in vitro* transcription of the sgRNAs: PxWhite: forward:TAATA CGACTCACTATAGGTCAGCGAGTTGAGGAGTGG TTTTAGAGCTAGAAATAGCAAGTTAA	This paper	N/A
Primer for obtaining the templates for *in vitro* transcription of the sgRNAs: PxABCG: TAATACGACTCACTATAGGAGCATCGC GACACTCGCTCGGTTTTAGAGCTAGA AATAGCAAGTTAAAATAAGGCTAGTCC	This paper	N/A

(*Continued on next page*)

Continued

REAGENT or RESOURCE	SOURCE	IDENTIFIER
Primer for obtaining the templates for *in vitro* transcription of the sgRNAs: reverse: AAAA GCACCGACTCGGTGCCACTTTTTCAAGTT GATAACGGACTAGCCTTATTTTAACTTGC TATTTCTAGCTCTAAAA	This paper	N/A
Primer for PCR in base insertion or deletion after genome editing: PxWhite: forward: CAAA CCCTTCACACCGACATT; reverse: CAATGAA CAGGTCCTGTTGTTG	This paper	N/A
Primer for PCR in base insertion or deletion after genome editing: PxABCG: forward:ACTTTATCC AAGCAAACCTCAGT; reverse: ACGCCAACGT AGTCACTTTTA	This paper	N/A
Software and algorithms		
TWOSEX-MSChar	Chi et al.[54]	http://140.120.197.173/Ecology/Download/Twosex-MSChart-exe-B100000.rar
SOAPnuke1.5.6	Chen et al.[55]	https://github.com/BGI-flexlab/SOAPnuke
Burrows-Wheeler Aligner BWA	Li and Durbin[56]	https://maq.sourceforge.net/
SAMtools	Li et al.[57]	https://maq.sourceforge.net/
RepeatMasker		www.repeatmasker.org
PoPoolation 1	Kofler et al.[58]	http://code.google.com/p/popoolation/
PoPoolation2	Kofler et al.[59]	http://code.google.com/p/popoolation2/
Bowtie2 v2.2.5	Langmead and Salzberg[60]	http://bowtie-bio.sourceforge.net/bowtie2/index.shtml
RSEM	Li and Dewey[61]	https://github.com/deweylab/RSEM/archive/v1.3.1.tar.gz
DESeq2	Love et al.[62]	http://www.bioconductor.org/packages/release/bioc/html/DESeq2.html.

RESOURCE AVAILABILITY

Lead contact

Further information and requests for resources should be directed to and will be fulfilled by the lead contact, Yanting Chen (fafucyt@126.com).

Materials availability

This study did not generate new unique reagents.

Data and code availability

- The source data is available as listed in the key resources table.
- No original code was generated for this paper.
- Any additional information required to reanalyze the data reported in this paper is available from the lead contact upon request.

EXPERIMENTAL MODEL AND STUDY PARTICIPANT DETAILS

Insect

The control strain of DBM, WT/CS, was obtained from the Institute of Zoology, Chinese Academy of Sciences (Beijing) in 2012. Since then, it has been maintained on artificial diet at a constant favorable temperature of 26°C in a climate incubator (DRX-400-DG, Ningbo Saifu Experimental Instrument CO., LTD, China). Approximately 1,000 control strain individuals were then kept under the elevated temperatures of 27°C for 12 h (dark) and 32°C for 12 h (light) in a climate incubator. The elevated temperature regimes utilized in this study were based on a study by Liu et al. that investigated the relationship between temperature and developmental rate in DBM, demonstrating their ability to survive and develop at temperatures of a maximum of 32°C.[63] Five replicate and independent hot-evolved populations were created. These hot-evolved

populations were originally from a favorable-temperature (26°C) population, which are genetically homogenous and maintained under the same temperature condition of 32°C for one year. They were therefore taken to be a single strain or and termed as the hot-evolved strain (HS).

METHOD DETAILS

Fitness parameters

The life tables of CS strain and the 1st, 5th, 10th, 20th and 30th generations of HS strain were established for investigating and comparing their development times, rates of survival, and rates of reproduction when maintained under favorable and high temperature conditions. Thirty newly laid eggs (< 12 h old) were placed in plastic Petri dishes (9 cm in diameter) with 3 replications (total 90 eggs), and then maintained under favorable and high temperature conditions. The three repeats were sampled from five hot-evolved populations. The number of larvae hatched from eggs was counted. Survival and development of each treatment was recorded every 12 h until all individuals died. The larvae were fed with artificial diet. After pupal emergence, all females and males in one repeat were transferred to plastic boxes for mating and laying eggs. Adults were provided with 10% honey. Eggs laid by females were counted every 12 h until all females died.

Life table data of CS and HS strains were analyzed using TWOSEX-MSChar.[54] The age-stage specific survival rate (s_{xj}), age-specific survival rate (l_x), age-specific fecundity (m_x), age-stage specific life expectancy (e_{xj}) and age-stage specific reproductive value (v_{xj}) were calculated.[64,65] The population parameters, including net reproductive rate (R_0), intrinsic rate of increase (r), finite rate (λ) and mean generation time (T), were also calculated. The variances and standard errors of these parameters were estimated using bootstrap technique with 100,000 times. Paired bootstrap tests were used to compare the difference between these parameters in CS and HS strains at a 5% significance level.

Responses to high temperature

Responses of CS and HS strains were tested using adults from the 56th generation. Female or male individuals emerged within 24 h were placed singly into 1.5 mL clear plastic vials (4.0 cm height) with a pinhole in the side wall for aeration. For each strain, twenty vials with females and twenty with males were then put into a plastic container (16.5 cm length, 11.5 cm width, 3.5 cm height). Four plastic containers with CS and four with HS DBM adults were placed into a climate incubator (DRX-400-DG, Ningbo Saifu Experimental Instrument CO., LTD, China) and subjected to one of the following heat shock treatments: 39°C, 40°C, 41°C, 42°C, 43°C, and 44°C, for 2 h. After each heat shock treatment, the plastic containers were removed from the climate incubator and placed in a temperature-controlled room at 26°C for 24 h, after which survival rate was recorded.

Logistic regression models were statistically fitted to the survival data to test the response of DBM to different temperatures. The results of the heat-shock experiment were numerically analyzed using the model log [p/(1−p)] = ajk + bjk T, where j is the strain (CS or HS), k is sex (male or female), and T is temperature (°C) used as a continuous predictor.

DNA sequencing, mapping, and data processing

Genomic DNA of CS and HS strain DBM was extracted for pool sequencing, respectively. The 33rd generation DBM of HS were sampled. For each population, DNA was extracted from 300 females with 10 replicates (30 females in each repeat). Two replicates were sampled for each evolved HS population (10 replicates in total). Genomic DNA was extracted using DNeasy Blood and Tissue Kit following the manufacturer's protocol (Qiagen, 69504). Genomic resequencing was performed with Illumina HiSeq 2000 at BGI, Shenzhen, China. Each sample was sequenced with a 10 × coverage. Sequencing libraries for each sample were constructed according to the manufacturer's protocol. SOAPnuke1.5.6 was used to eliminate the raw reads with adapters, unknown and low-quality bases, by the following parameters: -n 0.1 -l 20 -q 0.5 -Q 2 –G.[55] Trimmed sequences were mapping to the DBM reference genome using Burrows-Wheeler Aligner BWA.[56] The mapping results in SAM format were converted into BAM format using SAMtools[57] and filtered for a minimum mapping quality of 30. BAM files were transformed to pileup and mpileup files using SAMtools. Simple sequence repeats were identified using RepeatMasker (www.repeatmasker.org) with default sensitivity parameters but without interspersed repeats (option: -noint). Indels and 5 bp downstream and upstream every indel were identified using the script identify-genomic-indel-regions.pl from PoPoolation 1.[58] Then pileup files were converted to the PoPoolation2-specific sync format using the script mpileup2sync.jar from PoPoolation 2.[59] Indels and simple sequence repeats in sync files were subsequently removed using the script filter-sync-by-gtf.pl from PoPoolation 2.[59]

RNA sequencing and data analysis

Prior to RNA sequencing, the hot-evolved populations (the 33rd generation of HS, HS33) and CS were maintained at constant 26°C for two generations to eliminate environmental effects.[11] Individual pupae were placed into 1.5 mL clear plastic vials. Female adults emerging within 6 h were sampled and frozen in liquid nitrogen. For each strain, ninety vials with females were evenly put into three 1.5 mL tubes as three repeats (each tube with 30 females). All tubes with frozen moth samples were stored at -80°C before RNA extraction. Total RNA was extracted using Eastep® Super Total RNA Extraction kit (LS1040, Promega, USA), following the manufacturer's protocol. A NanoDrop Spectrophotometer (ND2000, Thermo Scientific, USA) and 2% agarose gel electrophoresis were used to determine the quality and quantity of RNA.

Transcriptome sequencing was performed with BGISEQ-500 at BGI, Shenzhen, China. mRNA libraries for each sample were constructed according to the manufacturer's protocol. Raw data with low quality, adaptor-polluted and high content (> 5%) of unknown base (N) reads were filtered using SOAPnuke1.5.6.[55] Clean reads were stored in FASTQ format. HISAT was used to preform *de novo* assembly with clean reads of high quality to obtain transcripts. Then Bowtie2 v2.2.5[60] was used to perform map clean reads to reference genome. Finally,

RSEM[61] was used to calculate the gene expression levels of genes and transcripts. Differentially expressed genes (DEGs) were identified using DESeq2[62] after adjustment for false-discovery rate (Q-values < 0.05). Gene Ontology (GO) enrichment and KEGG pathway analysis of DEGs were both implemented using phyper in R. The P values were adjusted by false discovery rate (FDR). The term with FDR less than 0.05 was defined as significant enrichment.

Identification of candidate genes

To identify genes likely to be differentiated, we used a two-pronged method to identify the most strongly differentiated alleles. The pairwise F_{ST} was calculated using the script fst-sliding.pl with the following parameters. The site with a read depth lower than 20 × and higher than 98% coverage were excluded from the analyses. A minor allele count of 6 was used as cutoff of SNPs to be called. To avoid increased stochastic error rates, F_{ST} was estimated for non-overlapping windows with setting window size and step size as 1000. Using the parameters described above, F_{ST} was also obtained for coding and non-coding regions. We then estimated the population parameter π to characterize genome wide patterns of variation and differentiation. Variance-sliding.pl in PoPoolation2 was used to estimate π. We assumed a minimum count of two, window size and step size of 1000 and used unbiased estimators for pooled data that corrected for pool size and coverage.[59,66] Further, snp-frequence-dif.pl was used to calculate the allele frequency differentiation across all SNPs. Only those falling into the upper 5% tail of the distribution were considered to be truly differentiated. The called SNPs were eventually subjected to two-sided Fisher's exact test (FET) using fisher-test.pl.

We defined candidate genes as those meet all the following criteria: (1) contained SNPs whose F_{ST}-value fell into the top 5% of the F_{ST} distribution; (2) contained SNPs whose π fell into the top 5% of the π distribution; (3) statistically significant allele frequency differentiation between populations with -log 10 (p-value) > 10; and (4) significantly different gene expression between CS and HS.

SNP mutant detecting

Nine females from the 44th generation of HS (HS44) were randomly selected from five independent hot-evolved populations to extract RNA. Total RNA was extracted using Eastep® Super Total RNA Extraction kit (LS1040, Promega, USA), following the manufacturer's protocol. The quality and quantity of RNA were determined by a NanoDrop Spectrophotometer (ND2000, Thermo Scientific, USA) and 2% agarose gel electrophoresis, respectively. cDNA was synthesized using GoScriptTM Reverse Transcription System (A5001, Promega Corporation, USA). PCR was performed with a 25 μL total reaction mixture, including 12.5 μL 2 × reaction buffer, 0.5 μL dNTP mix, 1.0 μL of primers (*PxWhite*: forward: 5′-ATGACGGCGGGAAATGAGGAGCAGGAGC-3′, reverse: 5′-TTATTTCGCCCTGCGCGTCCTCAGGACCAG-3′; *PxABCG*: forward: 5′-AGTGCGTCGTGCTATAGTGGG-3′, reverse: 5′-AGTGCGTCGTGCTATAGTGGG-3′), 0.5 μL DNase, 7.5 μL nuclease-free water, and 2.0 μL cDNA, using the Phanta Max Super-Fidelity DNA Polymerase (Vazyme, Nanjing, China). The PCR conditions were set as follow: 95°C for 5min; 35 cycles of 95°C for 15s, 70°C (*PxWhite*) / 61°C (*PxABCG*) for 15 s, 72°C for 2 min (*PxWhite*) / 1 min (*PxABCG*); and 72°C for 5min. PCR products were purified using Gel Extraction Kit (Omega, Morgan Hill, GA, USA) and then Sanger sequenced by Biosune Company (Fuzhou, China). Snap Gene software was used to compare the sequences of *PxWhite* and *PxABCG* between CS and HS. The allele frequencies of all SNPs in *PxWhite* and *PxABCG* were calculated to detect the mutant SNP.

Gene expression analysis

We used one control with CS DBM under favorable temperature at 26°C and four with CS DBM under four different temperature treatments. For the treatments, emerged adults were individually placed in a 1.5 mL plastic vial with a pinhole in the side wall and exposed to one of the following temperature treatments: two high-temperature treatments of 40°C for 30 min (H1) and 43°C for 30 min (H2); and two low-temperature treatments 4°C for 30 min (L1) and -17°C for 30 min (L2). Each temperature treatment and control included 15 vials with females and 15 vials with males. After each treatment, the vials were immediately frozen in liquid nitrogen and then stored at -80°C before RNA extraction.

Total RNA was extracted, and the quality and quantity of RNA were determined. Then cDNA was synthesized with 1.0 μg of total RNA. RT-qPCR was performed using the target gene-specific primers (*PxWhite*: forward: 5′-AGAAGTCATATCGGAGTTG-3′, reverse: 5′-GTATAA CATTCTGTGCCATAA-3′; *PxABCG*: forward: 5′-CAAGTTGGGTAGTGAGCTCGG-3′, reverse: 5′- ATGGAGAGCCGCTTGTACTGC-3′), which was designed using Oligo 7. The *PxRPL32* was as reference gene for normalization. RT-qPCR was conducted with a 20 μL total reaction mixture, including 2 μL cDNA, 0.4 μL of forward and reverse primer, 0.15 μL CXR reference dye, 7.05 μL nuclease-free water and 10 μL SYBR Green Supermix (A6001, Promega Corporation, USA) using QuantStudioTM 6 Flex real-time PCR system (ThermoFisher Scientific, USA). PCR conditions were set as follow: 95°C for 10 min, 40 cycles of 95°C for 15 s, 60°C for 30 s and then for a melt curve: 95°C for 15 s, 60°C for 1 min, 95°C for 15 s. The relative expression level of *PxWhite* and *PxABCG* in each treatment was normalized to the expression level of samples under control temperature, using $2^{-\Delta\Delta Ct}$ method.[67]

CRISPR/Cas9-based genome editing

The CS was used for functional validation of *PxWhite* and *PxABCG*. We selected sgRNA target sites 5′ - GGAGCATCGCGACACTCGCT - 3′ in *PxABCG* exon 3 and 5′ - GGTCAGCGAGTTGAGGAGTG - 3′ in *PxWhite* exon 3 according to the principle of 5′ - N_{20}NGG - 3′ (with the PAM sequence underlined). To obtain the templates for *in vitro* transcription of the sgRNAs, PCR was performed with a 50 μL total reaction mixture, including 25 μL 2 × buffer, 1.0 μL dNTP, 1.0 μL DNA polymerase, 1.5 μL of primer pairs (forward:5′-TAATACGACTCACTATAGGTCAGC GAGTTGAGGAGTGGTTTTAGAGCTAGAAATAGCAAGTTAA-3′ (*PxWhite*) / 5′-TAATACGACTCACTATAGGAGCATCGCGACACTCGC

TCGGTTTTAGAGCTAGAAATAGCAAGTTAAAATAAGGCTAGTCC-3′(*PxABCG*); reverse: 5′-AAAAGCACCGACTCGGTGCCACTTTTTCAAGTTGATAACGGACTAGCCTTATTTTAACTTGCTATTTCTAGCTCTAAAA-3′) and 20 μL nuclease-free water. PCR conditions were set as followed: 95°C for 3 min; 35 cycles of 95°C for 15 s, 68°C for 15 s, 72°C for 30 s, and then 72°C for 5 min. The PCR products were purified using Gel Extraction Kit (Omega, Morgan Hill, GA, USA). *In vitro* transcription was performed to generate sgRNAs using HiScribeTM T7 Quick High Yield RNA Synthesis Kit (New England Biolabs, Ipswich, MA, USA) in a 15 μL total reaction mixture, including 1.0 μL T7 RNA polymerase mix, 5.0 μL NTP buffer mix, 250 ng *in vitro* transcription templates of sgRNA, and added nuclease-free water to 15 μL. The reaction mixture was incubated under 37°C overnight. Then 1 μL DNase was added and incubated under 37°C for 30 min to get the sgRNA. The synthesized sgRNA was stored at -80°C for use after purification with phenol-chloroform extraction and ethanol precipitation.

For CRISPR knockout, a reaction mixture of 100 ng/μL Cas9 protein (GenCrispr, Nanjing, China), 300 ng/μL sgRNA, 0.5 μL 10× reaction buffer and adding nuclease-free water to 10 μL was first prepared. The mixture was then incubated under 37°C for 20 min. Fresh eggs, laid within 15 - 20 min, from WT females were injected with this mixture using an IM 300 Microinjector (Narishige, Tokyo, Japan). Microinjected eggs were then incubated at 26°C. The microinjected eggs that could successfully hatch and mature from larvae to adults were defined as G0. Newly emerged G0 adults were individually mated with control stain CST adults. After mated females laid eggs (G1), the gDNA of G0 moths were individually extracted using TiANamp Genomic DNA Kit (TIANGEN, China). Then PCR amplification with specific primers (*PxWhite*: forward: 5′-CAAACCCTTCACACCGACATT-3′, reverse: 5′- CAATGAACAGGTCCTGTTGTTG-3′; *PxABCG*: forward:5′-ACTTTATCCAAGCAAACCTCAGT-3′; reverse: 5′-ACGCCAACGTAGTCACTTTTA-3′) and sequencing were performed. The offspring of G0 with mutations were kept. The remaining G1 moths were paired individually to generate G2 progeny. When paired G1 female and male had the same allelic mutation (Aa), their offspring (G2) were preferentially kept. Three G2 lines could be generated, including no mutation (aa), mutation in single-strand DNA (Aa) and double-stranded DNA (AA). The remaining G2 moths were also paired individually to generate G3 progeny. When paired G2 female and male had the same lines (AA), their offspring (G3) were homozygous mutant, and considered to develop the homozygous mutant strain. If homozygous individuals could not be obtained in G3, mutation screening was continued to perform until obtaining the homozygous mutant strain (Pxwhite mutant strain (Pxwhite-MU) and PxABCG mutant strain (PxABCG-MU)).

Bioassay: Responses of mutant DBM to high temperatures

DBM strains used in this assay were CS, Pxwhite-MU and PxABCG-MU fourth instar larvae and adults. Twenty fourth instar larvae of CS, PxWhite-MU, and PxABCG-MU strains were put into a Petri dish (90 mm diameter). Then the Petri dishes were placed into the climate incubator where temperatures were set as 40°C, 41°C, 42°C, 43°C, and 44°C, for 2 h. Each treatment was repeated four times. After each heat shock treatment, the Petri dishes with larvae were removed from the climate incubator and placed in a temperature-controlled room at 26°C. The artificial diet was provided for the larvae. The number of larvae that could develop into pupae was recorded. The bioassay method for the adults was the same as the bioassay for responses of HS to high temperatures.

Eosin Y staining

To investigate the effect of *PxABCG* and *PxWhite* mutants on cuticle permeability, Eosin Y staining was performed on fourth instar larvae. Ten larvae were used for each strain. The larvae were put into a 2 mL microcentrifuge tube containing 1.5 mL dye solution (0.5% Eosin Y, PH0720, Scientific Phygene) and kept under 45°C for 2 h. Then, the larvae were washed using water until no Eosin Y was on the surface. Finally, the larvae were photographed with stereomicroscope (Lycra DMi8).